Author(s): Rumfeldt, Jessica; Takala, Heikki; Liukkonen, Alli; Ihalainen, Janne

Title: UV-Vis Spectroscopy Reveals a Correlation Between Y263 and BV Protonation States in Bacteriophytochromes

Year: 2019

Version: Accepted version (Final draft)

Please cite the original version:

Rumfeldt, J., Takala, H., Liukkonen, A., & Ihalainen, J. (2019). UV-Vis Spectroscopy Reveals a Correlation Between Y263 and BV Protonation States in Bacteriophytochromes. Photochemistry and Photobiology, 95(4), 969-979. https://doi.org/10.1111/php.13095

UV-Vis Spectroscopy Reveals a Correlation Between Y263 and BV Protonation States in Bacteriophytochromes

Supporting Information

Jessica A. Rumfeldt[1], Heikki Takala[1,2], Alli Liukkonen[1] and Janne A. Ihalainen,[1,*]

[1]University of Jyväskylä, Nanoscience Center, Department of Biological and Environmental Science, Jyväskylä, Finland

[2]University of Helsinki, Faculty of Medicine, Anatomy, Helsinki, Finland

*Corresponding author e-mail: janne.ihalainen@jyu.fi (Janne A. Ihalainen)

SUPPORTING RESULTS AND DISCUSSION

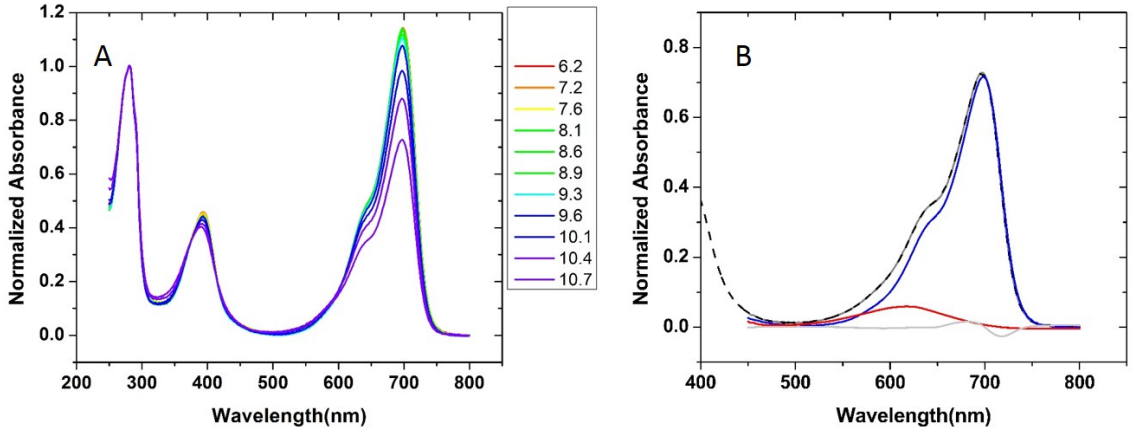

Figure S1: a) UV-Vis spectra as a function of pH for H290T b) Spectral decomposition. UV-Vis spectra of the Pr state at ~ pH 10.7 (dashed lines) are shown decomposed into components. For H290T two major components Comp1 and Comp2 (blue and red solid lines respectively) and a minor component (light grey line) are needed to reconstruct the spectra between 450 and 800 nm (shown as dark grey solid line).

pH reversibility of absorbance

The reversibility of BV absorbance upon decreasing the pH from pH 9.8 to ≤ 7.1 is 100%. For WT, when the initial pH is 10.4 the reversibility is 84% while for Y263F it is 95%. Thermodynamic analysis can therefore be performed on data obtained at pH 9.8 and below with less reliable pK_a values determined using data obtained above pH 9.8. This only applies to BV pK_a values of WT, H290T and Y263F which we state in the main text as having pK_a values above 10.

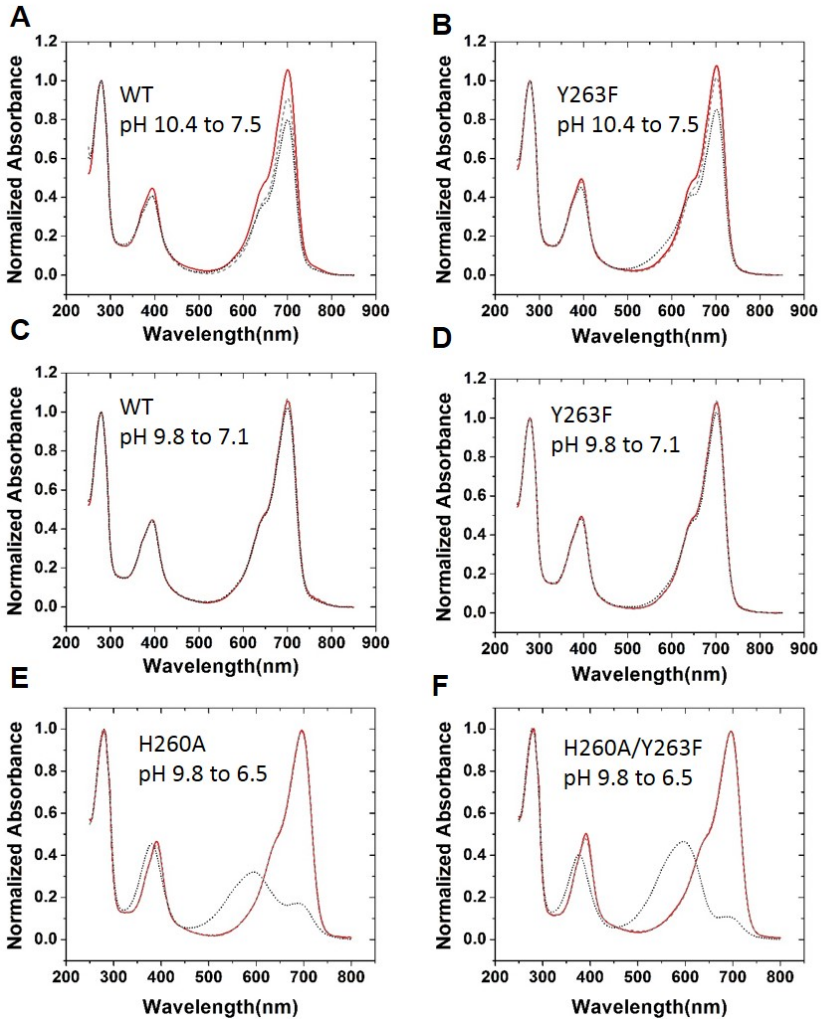

Figure S2. Reversibility of BV absorbance upon decreasing the pH from deprotonation to protonation conditions. The absorbance spectra of *Dr*-PSM when BV is protonated (red lines) is shown for A) WT and B) Y263F at pH 7.5, C) WT and D) Y263F at pH 7.1, and E) H260A and F) H260A/Y263F at pH 6.5. These are compared with spectra (dashed grey lines) in which the

specified construct was brought to the identical pH and protein concentration after an initial incubation in deprotonation conditions (10.4 or 9.8 as indicated on the graphs). Representative spectra of constructs in the deprotonated conditions are shown as dotted lines. Reversibility of the UV peak was 100% in all cases. Reversibility of the Q band for WT and Y263F from pH 10.4 to 7.5 was 84% and 95% respectively. Reversibility from 9.8 to 7.1(6.5) was 100% for WT, Y263F, H260A and H260A/Y263F.

BV geometry

There is no observable change in BV geometry due to pH as evidenced by absorbance of *Dr*-PSM after urea denaturation. The BV chromophore maintains the original geometry adopted in the native state after urea-induced denaturation (1). This phenomenon can be used to determine the amount of BV isomerization (2). At all pH values up to 10.6, there was no indication of BV isomerization indicating the increase in absorbance at 600 nm is not due to pH-induced isomerization.

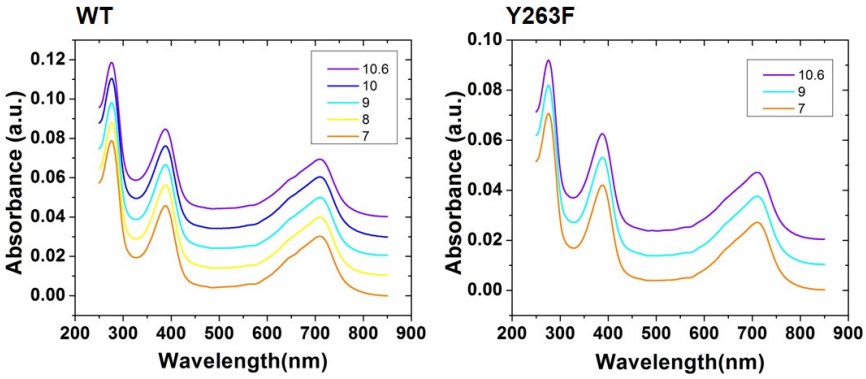

Figure S3. Maintenance of the Pr^{ZZZ} conformation of BV in high pH as indicated by Urea denaturation. Protein in pH buffered solutions (pH indicated on the graphs) was diluted into 10 M Urea pH 2.5 to obtain a final concentration of 8 M Urea.

Observation of Non-two-state behaviour in pH titration curves

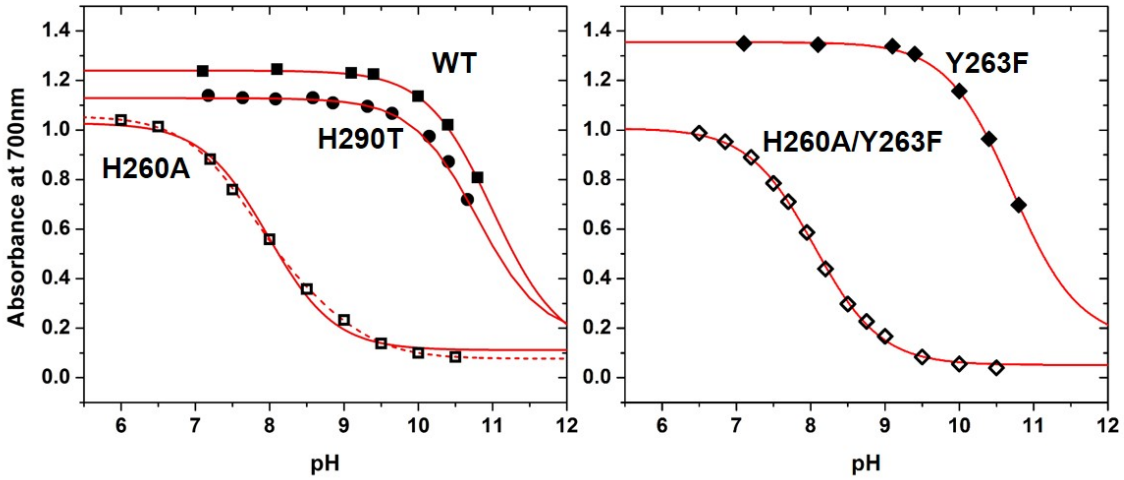

Figure S4: Plot of absorption at 700 nm as a function of pH for WT (solid squares), H290T (solid circles), H260A (open squares), Y263F (solid diamonds), H260A/Y263F (open diamonds). Solid red lines represent fits to a model with one pK_a while the dashed red line for H260A is a fit to the model with two pK_as.

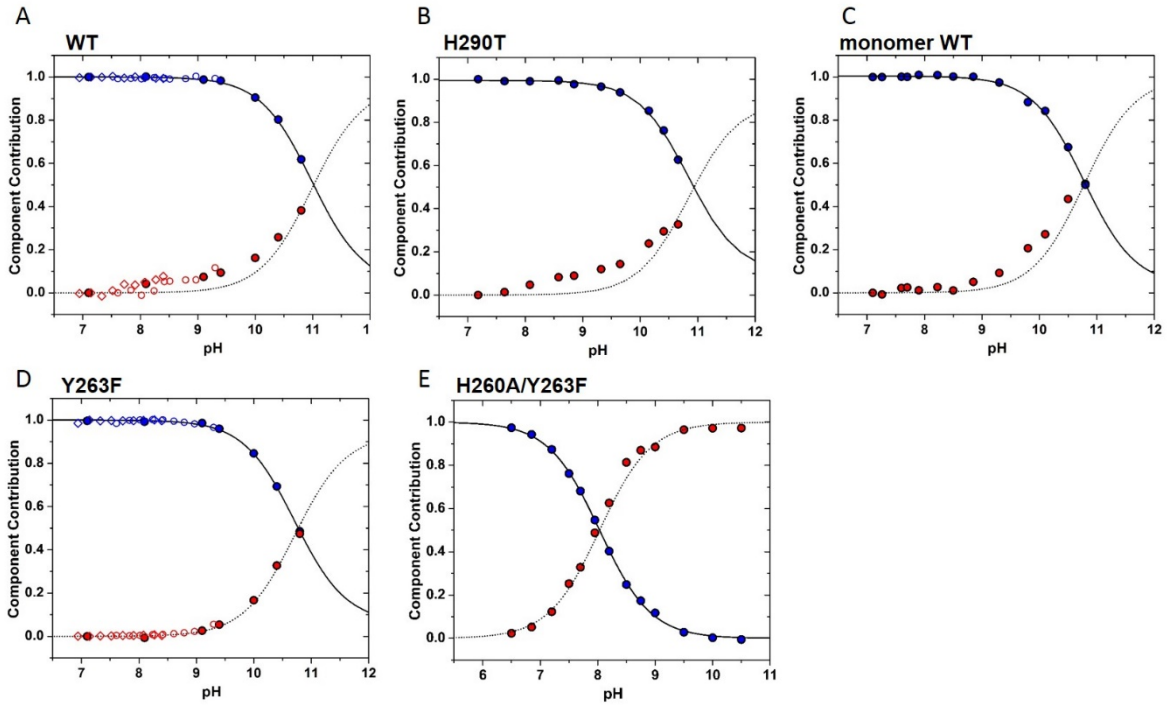

Figure S5. Deviation observed from a fit to one pK_a for a) WT b) H290T and c) monomer WT but not for d) Y263F or e) H260A/Y263F. The contribution of Comp1 shown as closed blue circles and Comp2 as closed red circles. The solid line is the single fit to one pK_a and the dotted line is its

reciprocal. For constructs with the Y263F mutation, the Comp1 and Comp2 component fractions as a function of pH are mirror images of each other with identical pK_a values. For WT and Y263F, the pH titration was also performed with Hepes (◇) and Bicine (○) buffer in the pH range 7 to 9.3 which shows that this trend is not buffer dependent.

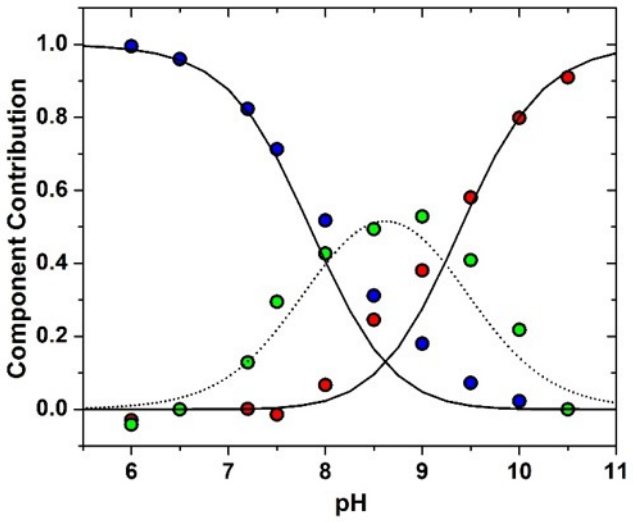

Figure S6. Global fitting of the major spectral components of H260A to the sequential 3-state model. There is deviation from the fit between pH 7.5 and 9.5. Symbols as in the main text Figure 4.

Direct evidence for Y263-OH deprotonation - absorbance and fluorescence in the UV region

In order to obtain direct evidence for Y263-OH deprotonation, the absorbance in the UV region was closely observed and analyzed (Figure S7 and S8, and Supporting Methods). The protonated and deprotonated absorbance spectra of free L-tyrosine in Figure S7(F) is similar to what has been observed previously for *N*-Acetyl-L-tyrosinamide (NATyrA) (3). The tyrosine difference spectra has a peak at 293 nm and a trough at 273 nm which is also observed in the difference spectra for all constructs at pH values of 10 or greater and most likely reflects deprotonation of one or more of the solvent exposed tyrosines which would have a pK_a value near 10.5 (4). The isosbestic points

observed in Figure S7 at 280 nm are artifacts of the normalization method. The deprotonation of NATyrA has isosbestic points at 269 and 278 nm (3).

For constructs with Y263, the difference spectra at low pH (pH 7 to 9) has a different appearance than those at higher pH values, with a peak centered at 301 nm and a small trough at 286 nm.(Figure S7B,C,E) For constructs with the Y263F mutation, the difference spectra at the same pH values (pH 7 to 9) do not show the same peak at 301 nm.(Figure S7A,D) Together, this is interpreted as evidence for Y263-OH deprotonation with influence of BV and binding site amino acid side-chains altering the absorption properties of the tyrosinate.

The ΔAbsorbance at specific wavelengths are plotted as a function of pH in Figure S8 along with the fraction of Y263-O^- {([BA] + [BB])/([AA] + [AB] + [BA] + [BB])} calculated assuming the four-state model in Figure 5 and the pK_a values in Table 2. In A) Y263F, WT and H290T and B) H260A/Y263F and H260A are plotted the ΔAbsorbance averaged for 300 – 302 nm. The constructs with Y263 (red symbols) show a larger ΔAbsorbance in the pH range between 7 and 10 than those with the Y263F mutation (black symbols) indicating that Y263 is deprotonating. In panels C) Y263F, WT and H290T and D) H260A/Y263F and H260A the ΔAbsorbance at 293 nm shows relatively little change until pH 10 for all but H260A which shows a small gradual increase in this region. As observed in the difference spectra, this is consistent with an initial deprotonation of Y263-OH between pH 7 and 10 with subsequent deprotonation of solvent exposed tyrosines after pH 10. The theoretical absorbance at 300-302 nm and 293 nm at pH 9 can be calculated using tyrosine difference spectra in Figure S7(F) and Figure S8(E). Using these values, data from WT, H290T and H260A are not completely consistent with one tyrosine deprotonation per monomer below pH 10 which may be due to influence of nearby charges as discussed above.

Since deprotonation of tyrosine results in an increased fluorescence at 340 nm,(5) fluorescence measurements were also carried out to provide additional direct evidence for Y263-OH deprotonation.(Figure 8) The emission spectra (excitation at 275 nm) are plotted in Figure S9A for WT and Y263F and S9B for H260A and H260A/Y263F. Note that the concentration of WT and Y263F is ~ 4 μM and the concentration of H260A and H260A/Y263F is ~ 2.2 μM. Except for Y263F, fluorescence intensity is greater at pH 8.9 (dashed lines) than at pH 7.1 (solid lines). The difference spectra (pH 8.9 minus pH 7.1) are shown in C) for WT and Y263F and D) H260A and H260A/Y263F. From this it can be seen that the pH-induced fluorescence increase is larger for WT and H260A constructs than for their corresponding tyrosine mutations, Y263F and H260A/Y263F. The ΔΔFluorescence spectra are plotted in S9 E) ΔWT minus ΔY263F and F) ΔH260A minus ΔH260A/Y263F. Using Figure S8(E) the increase in the fractional population of Y263-O^- from pH 7.1 to 8.9 is 0.72 for WT and 0.25 for H260A. From this and the difference in protein concentration, it is expected that the ΔΔFluorescence of WT should be ~5 times higher than for H260A which is similar to what is observed. Therefore, both UV-absorbance and fluorescence are consistent with Y263-OH deprotonation.

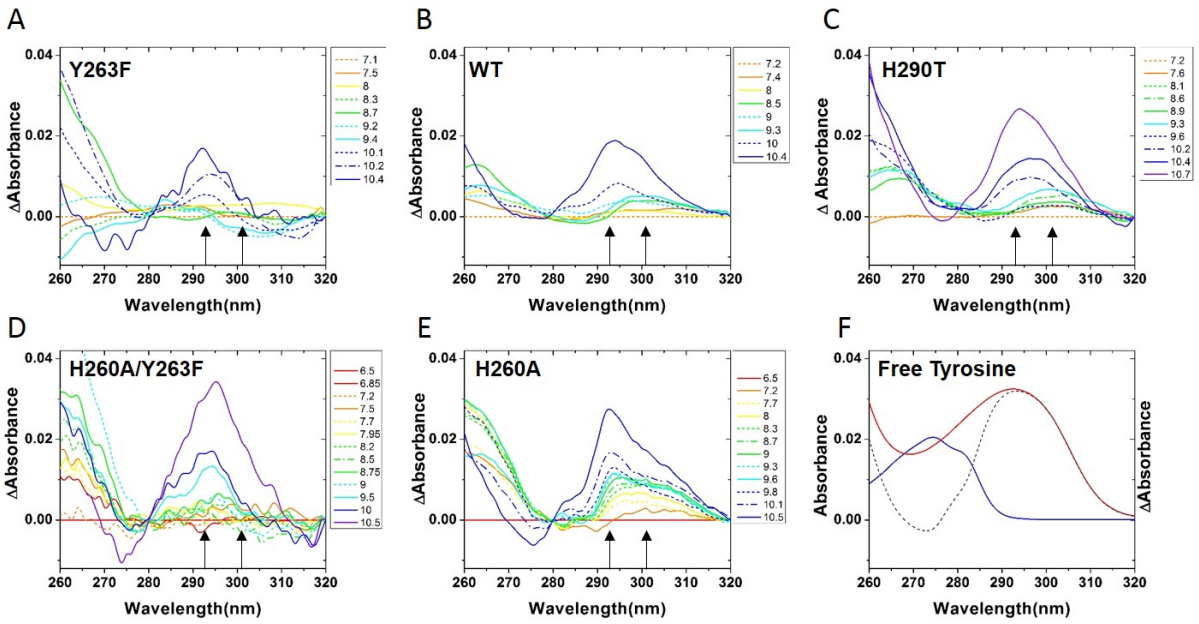

Figure S7. Changes in UV-absorption as a function of pH. For a given construct, the UV region of the absorption spectra (250 – 320 nm) was normalized as outlined in supporting methods. The spectrum measured at the lowest pH (6.5 to 7.2) was then subtracted from the spectra measured at the higher pH values (pH values indicated beside the graphs). The resulting difference spectra are shown in A) for Y263F, B) WT C) H290T D) H260A/Y263F and E) H260A. Traces have been smoothed for clarity. For comparison, the spectra of free L-tyrosine in solution is shown in F) fully protonated (blue), deprotonated (red) as well as the difference spectra, deprotonated minus protonated (dashed grey line). The absorbance of these traces have been scaled to correspond to one tyrosine per monomer of *Dr*-PSM (see Supporting Information Methods).

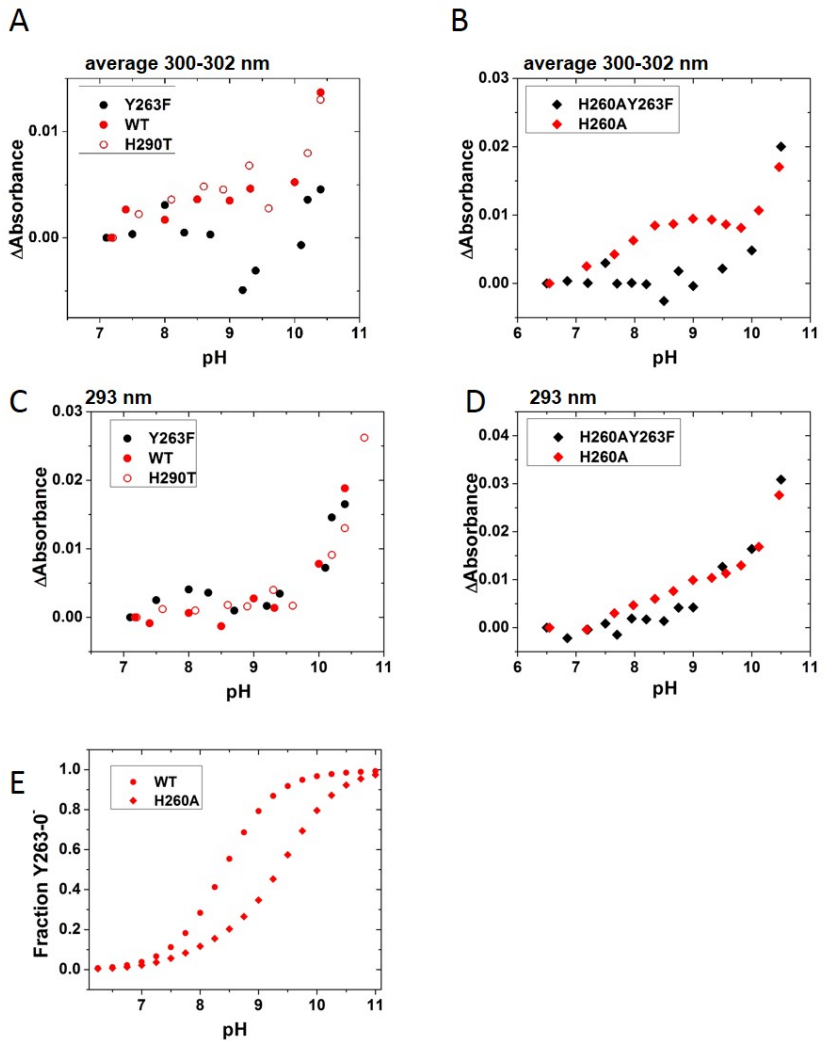

Figure S8. Plots of the absorption difference at the specific wavelength regions indicated by arrows in Figure S7. The absorbance difference averaged for wavelengths 300 to 302 nm is plotted in A) for Y263F, WT and H290T and in B) for H260A/Y263F and H260A. The absorption difference in this region for constructs with Y263: WT, H290T, H260A (red symbols), shows an increase relative to Y263F and H263A/Y263F (black symbols) starting after pH 7. The absorbance difference at 293 nm as a function of pH is shown in C) for Y263F, WT and H290T and in D) for H260A/Y263F and H260A. In E, the fraction of Y263-O^- as a function of pH is shown for WT (circles) and H260A (diamonds) which has been calculated using the model in Figure 5 in the main text (i.e. species BA + BB) and the corresponding pK_a values in Table 2 main text.

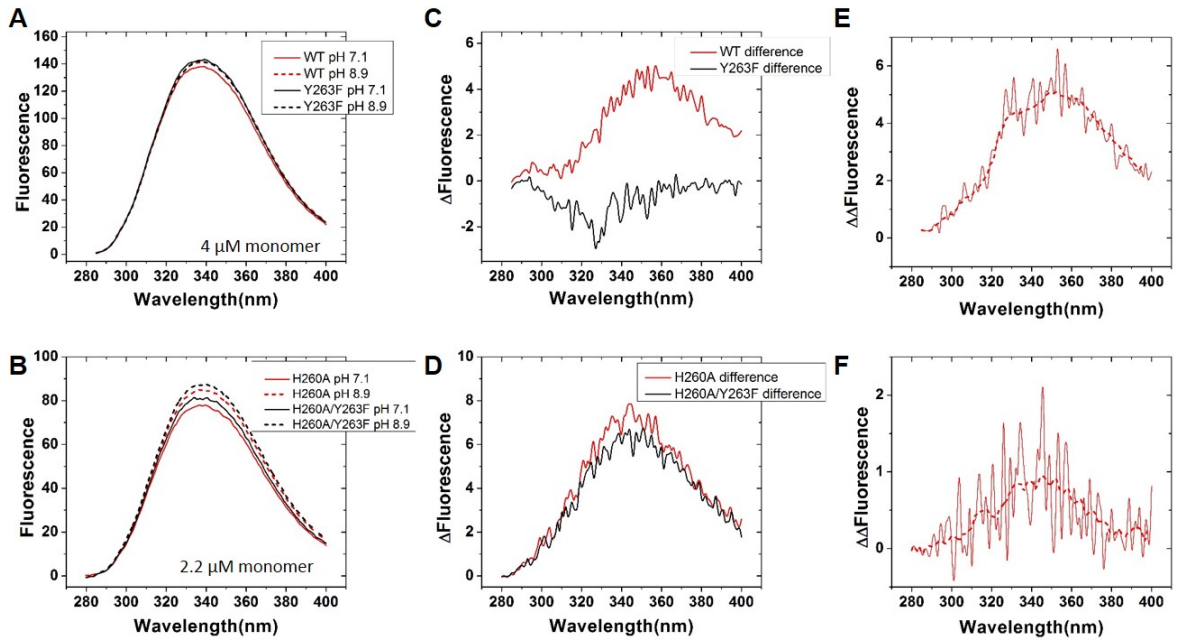

Figure S9. UV Fluorescence at pH 7.1 (solid lines) and pH 8.9 (dashed lines) of A) WT (red lines) and Y263F (black lines) and B) H260A (red lines) and H260A/Y263F (black lines). The difference spectra (pH 8.9 minus pH 7.1) is shown in C) for WT (red) and Y263F (black) and D) for H260A (red) and H260A/Y263F (black). The double difference spectra are shown for WT in E) (WT difference minus Y263F difference) and for H260A (H260A difference minus H260A/Y263F difference) in F. The sold lines are raw ΔΔFluorescence and the dashed lines represent the smoothed data.

Error Estimation

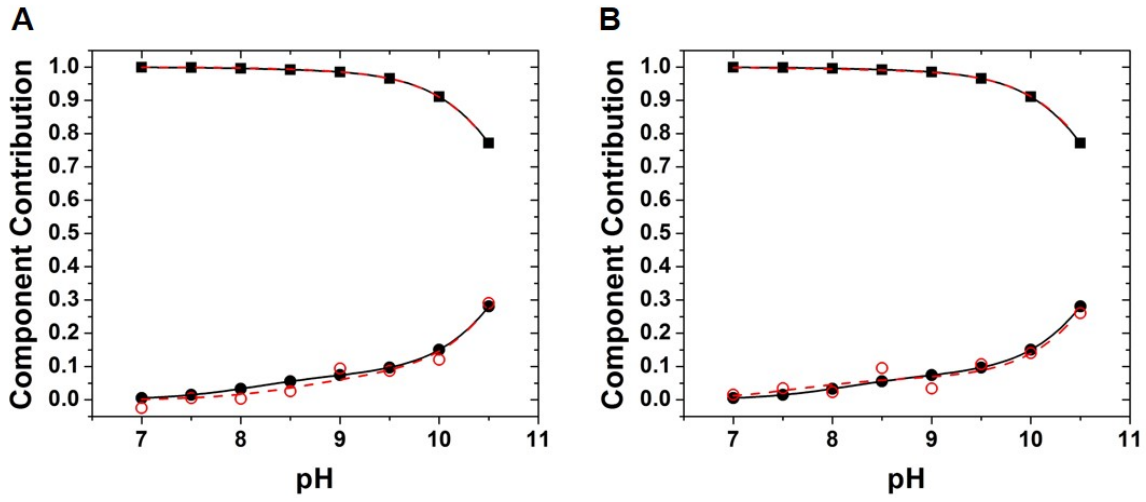

Figure S10. Error estimation. Data was generated using the four pK_a model (Equation 1) and pK_a1 2, 3 and 4 values of 10.2, 11.0, 8.1 and 8.9 respectively (black symbols). Using this ideal data, the fitted values converged to the same pK_a values used to generate the data (solid black lines). Noise

was then added to Comp2 (red symbols) using a random number generator. Specifically, integer values from -3 to +3 or -4 to +4 were generated for each data point which indicated the addition of -0.03 to 0.03 (A) or -0.04 to 0.04 (B) respectively. In A) the fitted pK_a1, 2, 3 and 4 values are 10.5, 11.0, 8.6 and 9.1 respectively. In B) the fitted pK_a1, 2, 3 and 4 values are 9.7, 11.1, 7.6 and 8.9 respectively. From this is appears that noise in the data has a larger contribution to errors in pK_a than the inability to include data beyond pH 10.5. This error is estimated to be ± 0.5 pH units.

Tables

Table S1. Wavelength maxima determined from UV-Vis spectra of *Dr*-PSM variants in Pr

	Dark Pr^{ZZZ}			
	Low pH		High pH	
CBD-PHY	Soret	Q	Soret	Q
WT	395	701	391	631
Y263F	396	702	391	616
H290T	393	698	391	620
H260A	390	696	381	600
H260A/Y263F	391	696	377	598

The Q band wavelength at high pH taken from spectral component Comp2

Table S2. Parameters determined from fitting spectral components to models involving one to two pK_a values.

Protein			BV	Y263-OH
Dr-PSM	Data Set[a]	Fit[b]	pK_{a1}	pK_{a3}
WT[c]	C1	S-1pK_a	10.9	-
	C1 & C2	G-2pK_a	10.9	8.4
H290T[c]	C1	S-1pK_a	10.6*	-
	C1 & C2	G-2pK_a	10.7	8.3
H260A[d]	C1, C2, C3	-	-	-
Y263F	C1	S-1pK_a	10.6	-
H260A/Y263F	C1	S-1pK_a	8.0	-

[a] C1, C2, C3 are the components Comp1, Comp2 and Comp3 used to deconvolute the spectra

[b] S and G refer to the single or global fit respectively of the component(s) in the data set with one or two pK_as. For the single fit, pK_{a1} refers to the pK_a for BV deprotonation. For global fits, the pK_a values 1 and 3 correspond to those outlined in the model in Figure 5 of the main text. Standard errors from Origin fitting ranged from 0.3 to 4 % of the fitted value. The pK_a values reported in the table are an average from fits to two separate titrations. The 95% confidence interval was in general 0.2 pH units except values with asterisks* which had 95% confidence intervals between 0.4 and 0.6

[c] For WT and H290T, although C1 can be individually fit with one pK_a, global fits of C1&C2 require at least two pK_a values. The global fit with 4 pK_as is reported in the main text.

[d] Individual fits of H260A components require at least two pK_as but do not provide meaningful information. The best fit to the data is with the four pK_a model reported in the main text.

SUPPORTING METHODS

Reversibility Measurements

Dr-PSM was added to 30 mM Glycine (pH 10.4 and/or 9.8) and a final concentration of 4 μM monomer and then diluted 1:1 into 60 mM Mes buffer (pH 5.5 to pH 6.2) and the absorption spectra was measured. The final pH of the sample as reported was then measured with a pH meter. Spectra were scaled to an absorbance at 280 nm of 1. In order to determine the reversibility, the absorbance spectra of constructs were also measured in pH 6.5, 7.1 and 7.5 buffer (i.e. the same conditions determined after dilution from high into low pH). The absorbance at 280 nm and 700 nm were used to calculate percent reversibility: 100 × (absorbance after dilution from high to low pH) ÷ (absorbance in low pH). Spectral decomposition was also used to compare the shape of the Q band (450 to 800 nm) using SPLAB (6).

UV absorbance

Absorption spectra were scaled so that the absorption at 320 nm was set to zero and the value at 280 nm was set to 1. The spectrum measured at the lowest pH, which was in the range of pH 6.5 to 7.2, was then subtracted from the spectra measured at the higher pH values. These difference spectra are plotted in Figure S8. The averaged Δabsorbance using values at 300, 301 and 302 nm as well as the single Δabsorbance value at 293 nm were plotted as a function of pH in Figure S9. Since the protein spectra have been normalized to an absorbance at 280 nm of 1, the apparent protein concentration is then 13.5 μM monomer using a theoretically calculated extinction coefficient of 73 910 M^{-1} cm^{-1} at 280 nm.(7) The protonated tyrosine spectra was obtained using 1 mL of 0.1 mM solution of L-Tyrosine (Sigma Aldrich) in water. The spectrum did not change after adding 2 μL of 1 M HCL. The deprotonated spectra was obtained by adding 6 μL of 1 M NaOH.

The spectrum did not change upon further additions of NaOH. The spectra are normalized to 13.5 μM in Figure S8(F) using an extinction coefficient of the protonated form of 1280 $M^{-1}cm^{-1}$ at 280 nm and a 1 cm path length cuvette. The difference spectrum was obtained by subtracting the protonated from the deprotonated spectrum. This then corresponds to the absorbance difference of one tyrosine per monomer of *Dr*-PSM when the protein spectrum is normalized using 280 nm equal to 1.

Fluorescence Measurements

Fluorescence emission experiments were carried out using a Cary Eclipse fluorescence spectrophotometer. Excitation wavelength was set to 275 nm with excitation and emission monochromator band paths set to 2.5 nm. The scan rate was 120 nm/min with 1 nm data intervals and 0.5 s averaging time. Each scan was repeated five times and then averaged. Measurements were carried out in 30 mM Tris buffer pH 7.1 and 8.9 at 4 μM monomer for WT and Y263F and 2.2 μM monomer H260A and H260A/Y263F. The absorbance spectra was measured before and after fluorescence which confirmed there was no change in absorbance due to the fluorescence measurement. The UV absorbance region (250 to 320 nm) was used to normalize the fluorescence using spectral decomposition with the spectra of WT pH 7.1 as the standard and a first order polynomial baseline to account for slight differences in scattering. The reported multiplication factor (1.01 to 0.97) was then used to normalize the fluorescence spectra measured with different constructs and pH values. Each full absorbance and fluorescence experiment was carried out two times and the resulting spectra averaged.

Models used for fitting pH titration data

The simplest case involves one titration group and can be considered a two-state model between protonated and deprotonated forms:

$$\boldsymbol{X}H^+ \overset{K_a}{\leftrightarrow} \boldsymbol{X} + H^+ \qquad \text{Equation S1}$$

In equation S1, the protonated and deprotonated forms are shown as $\boldsymbol{X}H^+$ and $\boldsymbol{X}$ respectively, but, can also be written as $\boldsymbol{X}H$ and X^-, H^+ is the proton which has a positive charge and K_a is the equilibrium constant:

$$K_a = \frac{[\boldsymbol{X}][H^+]}{[\boldsymbol{X}H^+]} \qquad \text{Equation S2}$$

Equation S2 can be rearranged to give the Henderson Haselbach equation:

$$pH = pK_a + log\,\frac{[\boldsymbol{X}]}{[\boldsymbol{X}H^+]} \qquad \text{Equation S3}$$

Using Equation S3, the fraction of the protonated and deprotonated groups at a given pH are

$$f\boldsymbol{X}H^+ = \frac{\boldsymbol{X}H^+}{\boldsymbol{X}+\boldsymbol{X}H^+} = \frac{1}{10^{(pH-pK_a)}+1} \qquad \text{Equation S4a}$$

$$f\boldsymbol{X} = \frac{X}{\boldsymbol{X}+\boldsymbol{X}H^+} = \frac{1}{1+10^{(pK_a-pH)}} \qquad \text{Equation S4b}$$

The total signal (determined by absorbance or by component analysis) is the sum of the fraction of each species in solution multiplied by their individual signals.

$$S = S_a(f\boldsymbol{X}H^+) + S_b(f\boldsymbol{X}) \qquad \text{Equation S5}$$

Where S is the signal determined at a given pH, S_a/S_b is the signal associated with $\boldsymbol{X}H^+/\boldsymbol{X}$ which corresponds to the value at the low/high pH titration endpoint.

Since the sum of the fraction of all species in solution is equal to 1, Equation S5 can be cast using the total change in absorbance or component contribution during titration given, $\Delta S = S_a - S_b$:

$$S = S_b + \Delta S \frac{1}{10^{(pH-pKa)}+1}$$ Equation S6a

Deviation from this fit may indicate the presence of more than one titration group. Fitting to the Hill equation below can give an unbiased assessment of the applicability of fitting to a more complex model.

$$S = S_b + \Delta S \frac{(10^{-pH})^n}{(10^{-MP})^n+(10^{-pH})^n}$$ Equation S6b

Where *n* is the Hill coefficient (a value of 1 indicates a single species is being titrated and values above or below indicate that more than one pH dependent process is taking place), *MP* is the midpoint in pH units of the pH titration, which, when the Hill coefficient is 1, is equal to the pK_a.

For a three-state model that involves two titration groups, the following equation can be used for fitting:

$$S = \frac{\Delta S_1}{1+10^{(pKa1-pH)}} + \frac{\Delta S_2}{1+10^{(pKa2-pH)}} + S_a$$ Equation S7

In Equation S7, the two pK_a values, pK_{a1} and pK_{a2}, with corresponding amplitude changes ΔS_1 and ΔS_2 are assumed to be from two completely independent titrations.(8)

For phytochrome, titration groups can be from BV, nearby amino acids that influence BV absorbance, or, a combination of the two. If the two titration groups are considered to be from the same phytochrome monomer subunit, the following thermodynamic cycle can be drawn:

$$\begin{array}{ccc} \boldsymbol{X}HY\boldsymbol{H}^+ & \overset{K_{a1}}{\longleftrightarrow} & \boldsymbol{XY}H + H^+ \\ K_{a3} \updownarrow & & \updownarrow K_{a4} \\ \boldsymbol{X}HY + H^+ & \overset{K_{a2}}{\longleftrightarrow} & \boldsymbol{XY}^- + 2H^+ \end{array}$$ Equation S8

Where $\boldsymbol{X}$ and $\boldsymbol{Y}$ are the two titration groups. If $K_{a3} << K_{a1}$ and K_{a4}, the deprotonation events are sequential such that $\boldsymbol{X}$ deprotonates before $\boldsymbol{Y}$. In this case the equation simplifies to:

$$\boldsymbol{XHYH}^{+} \overset{K_{a1}}{\leftrightarrow} \boldsymbol{XYH} + H^{+} \overset{K_{a4}}{\leftrightarrow} \boldsymbol{XY}^{-} + 2H^{+} \qquad \text{Equation S9}$$

Using Equations 2 and 3:

$$pH = pK_{a1} + log\frac{[\boldsymbol{XYH}]}{[\boldsymbol{XHYH}^{+}]} = pK_{a4} + log\frac{[\boldsymbol{XY}^{-}]}{[\boldsymbol{XYH}]} \qquad \text{Equation S10}$$

The fraction f of each species is equal to:

$$f\boldsymbol{XHYH}^{+} + f\boldsymbol{XYH} + f\,\boldsymbol{XY}^{-} = 1 \qquad \text{Equation S11}$$

From equations 10 and 11

$$f\boldsymbol{XYH} = \frac{1}{\frac{1}{10^{(pH-pK_{a1})}} + 10^{(pH-pK_{a4})} + 1} \qquad \text{Equation S12a}$$

$$f\boldsymbol{XHYH}^{+} = \frac{f\boldsymbol{XYH}}{10^{(pH-pK_{a1})}} \qquad \text{Equation S12b}$$

$$f\boldsymbol{XY}^{-} = \frac{f\boldsymbol{XYH}}{10^{(pH-pK_{a4})}} \qquad \text{Equation S12c}$$

From the fraction of each species in Equations 12a-c, the total signal can then be written as in Equation S5 using *S,* the signal associated with each species and an additional scaling factor, F.

$$S = F_{\boldsymbol{XHYH}^{+}}[S_{\boldsymbol{XHYH}^{+}}(f\boldsymbol{XHYH}^{+})] + F_{\boldsymbol{XYH}}[S_{\boldsymbol{XYH}}(f\boldsymbol{XYH})] + F_{\boldsymbol{XY}^{-}}[S_{\boldsymbol{XY}^{-}}(f\boldsymbol{XY}^{-})]$$

Equation S13

The scaling factors $F_{\boldsymbol{XHYH}^{+}}$, $F_{\boldsymbol{XYH}}$ and $F_{\boldsymbol{XY}^{-}}$ are needed when globally fitting multiple data sets as they set how much each species contributes to the signal being fit. For example when globally fitting three components, the pK_a and S values are shared across all data sets while each component is fit with one scaling factor set to 1 and the other two to 0.

If the two titration groups in Equation S8 deprotonate in parallel, then $K_{a1} + K_{a4} = K_{a2} + K_{a3,}$ and the fraction f of each species is equal to:

$$f\boldsymbol{XHYH}^{+} + f\boldsymbol{XYH} + f\boldsymbol{XHY} + f\,\boldsymbol{XY}^{-} = 1 \qquad \text{Equation S14}$$

From Equations S2, S3 and S11:

$$f\boldsymbol{XY}H = \frac{1}{\frac{1+10^{(pH-pK_{a3})}}{10^{(pH-pK_{a1})}}+10^{(pH-pK_{a4})}+1}$$ Equation S15a

$$f\boldsymbol{X}H\boldsymbol{Y}H^{+} = \frac{f\boldsymbol{XY}H}{10^{(pH-pK_{a1})}}$$ Equation S15b

$$f\boldsymbol{XHY} = f\boldsymbol{X}H\boldsymbol{Y}H^{+} \times 10^{(pH-pK_{a3})}$$ Equation S15c

$$f\boldsymbol{XY}^{-} = f\boldsymbol{XY}H \times 10^{(pH-pK_{a4})}$$ Equation S15d

Using Equations S15a-d, the total signal can be written as described for Equation S13:

$$S = F_{\boldsymbol{X}H\boldsymbol{Y}H^{+}}[S_{\boldsymbol{X}H\boldsymbol{Y}H^{+}}(f\boldsymbol{X}H\boldsymbol{Y}H^{+})] + F_{\boldsymbol{XY}H}[S_{\boldsymbol{XY}H}(f\boldsymbol{XY}H)] + F_{\boldsymbol{X}H\boldsymbol{Y}}[S_{\boldsymbol{X}H\boldsymbol{Y}}(f\boldsymbol{X}H\boldsymbol{Y})] + F_{\boldsymbol{XY}^{-}}[S_{\boldsymbol{XY}^{-}}(f\boldsymbol{XY}^{-})]$$ Equation S16

REFERENCES

1. Hirose, Y., N. C. Rockwell, K. Nishiyama, R. Narikawa, Y. Ukaji, K. Inomata, J. C. Lagarias and M. Ikeuchi. (2013) Green/red cyanobacteriochromes regulate complementary chromatic acclimation via a protochromic photocycle. *Proc. Natl. Acad. Sci. U. S. A.* **110**, 4974-4979.

2. Lenngren, N., P. Edlund, H. Takala, B. Stucki-Buchli, J. Rumfeldt, I. Peshev, H. Hakkanen, S. Westenhoff and J. A. Ihalainen. (2018) Coordination of the biliverdin D-ring in bacteriophytochromes. *Phys. Chem. Chem. Phys.* **20**, 18216-18225.

3. Melo, E. P., M. R. Aires-Barros, S. M. Costa and J. M. Cabral. (1997) Thermal unfolding of proteins at high pH range studied by UV absorbance. *J. Biochem. Biophys. Methods* **34**, 45-59.

4. Grimsley, G. R., J. M. Scholtz and C. N. Pace. (2009) A summary of the measured pK values of the ionizable groups in folded proteins. *Protein Sci.* **18**, 247-251.

5. Maeno, A., H. Matsuo and K. Akasaka. (2013) Tyrosine/tyrosinate fluorescence at 700 MPa: A pressure unfolding study of chicken ovomucoid at pH 12. *Biophys. Chem.* **183**, 57-63.

6. Davydov, D. R., E. Deprez, G. H. Hoa, T. V. Knyushko, G. P. Kuznetsova, Y. M. Koen and A. I. Archakov. (1995) High-pressure-induced transitions in microsomal cytochrome P450 2B4 in solution: Evidence for conformational inhomogeneity in the oligomers. *Arch. Biochem. Biophys.* **320**, 330-344.

7. Wilkins, M. R., E. Gasteiger, A. Bairoch, J. C. Sanchez, K. L. Williams, R. D. Appel and D. F. Hochstrasser. (1999) Protein identification and analysis tools in the ExPASy server. *Methods Mol. Biol.* **112**, 531-552.

8. Nielsen, J. E. (2009) Chapter 9 Analyzing Enzymatic pH Activity Profiles and Protein Titration Curves using Structure-Based pKa Calculations and Titration Curve Fitting, in pp 233-258, Elesvier Inc, .